Journal of Theoretical and Applied Physics (JTAP), Special Issue: AICIS'23-Article 11

Proceeding of the 3rd Annual International Conference on Information and Sciences 2023, University of Fallujah, Iraq

https://dx.doi.org/10.57647/j.jtap.2024.si-AICIS23.11

Preparation of titanium dioxide NPs and study of optical parameters as a polymer photocatalytic film

Rasheed Lateef Jawad[1,2,*], Raghad Subhi Abbas[1]

[1]*Department of Physics, College of Education for Pure Science Ibn Al-Haitham, University of Baghdad, Baghdad, Iraq.*
[2]*Al-Karkh University of Science, Baghdad, Iraq.*

[*]**Corresponding author:** rasheed.jawad2104p@ihcoedu.uobaghdad.edu.iq

Original Research

Published online:
15 June 2024

Abstract:

In this study, titanium dioxide (TiO_2) nanoparticles are combined with a mixture of polymers (polyvinyl-alcohol PVA, polyethylene-glycol PEG and polyvinylpyrrolidone PVP). Titanium dioxide (TiO_2) NPs was formulation by sol-gel process, nanocomposites were prepared with concentration (1, 5, 10, 15, 20 and 25 wt%). TiO_2 NPs after subjecting them to a calcination process at a temperature of about 400 °C and 700 °C and polymer blend of different concentrations (PVA various wt%, PEG constant wt% and PVP constant wt%). A UV-Vis spectrometer was used to determine the optical constants of the prepared-samples. Absorption coefficient, extinction coefficient, refractive-index and optical energy-gap were calculated, it was noticing of absorption coefficient values in calcination 400 °C for 25 wt% TiO_2 NPs higher than that of other samples. The refractive index of TiO_2 at 700 °C is higher than that of 400 °C due to the different crystalline structure of rutile. The optical energy band gap was determined and it was discovered to decrease from 5.16 eV for (1 wt% TiO_2) blended with (PVA 84 wt%, PEG 10 wt% and PVP 5 wt%) up to 3.51 eV (25 wt% TiO_2) with concentrations of (PVA 60 wt%, PEG 10 wt% and PVP 5 wt%) as matrix. At a higher calcination temperature of 700 °C, TiO_2 transitions from the anatase phase to the rutile phase, this change in crystal structure has a significant effect on the value optical dielectric constant real part (ε_r) which is (16.06). The findings have important ramifications for possible uses these nanocomposites to enable reuse of the photocatalysts, thus extending their useful life.

Keywords: Titanium dioxide nanoparticles; PVA; PEG; PVP; Optical constant; Polymer blend

1. Introduction

Nanocomposites have emerged as a prominent field of study, holding immense potential for various applications. The utilization of polymers in nanomaterials synthesis has been extensively explored owing to their remarkable properties. Titanium dioxide, also known as titania (TiO_2), is a white material that is widely used in environmental photocatalysis, self-cleaning and anti-fogging surfaces, and photo electrochemical conversion of solar energy [1]. Titanium dioxide nanoparticles are among the most widely used nanomaterials due to their distinctive optical and chemical characteristics.

The addition of Nano titanium oxide (TiO_2) to polyvinyl alcohol (PVA) enhances the photocatalytic properties for water purification. TiO_2, when in nano form, has a larger surface area, improving its photocatalytic efficiency. When exposed to UV light, TiO_2 generates electron-hole pairs, which can react with water molecules or organic contaminants, leading to the formation of reactive oxygen species (ROS) like hydroxyl radicals. These ROS can decompose organic compounds in water [2].

PVA serves as a stable support for TiO_2 nanoparticles, preventing aggregation and ensuring uniform dispersion. It also provides mechanical strength and flexibility to the composite material, making it durable and suitable for practical use. Furthermore, PVA enhances the absorption of visible light, expanding the photocatalytic activity of TiO_2 to the visible light spectrum [3].

In summary, the combination of Nano TiO_2 and PVA in a composite material offers improved photocatalytic properties [4], enabling the degradation of organic pollutants and the inactivation of microorganisms in water, making it a

promising solution for water purification.
However, these nanoparticles (NPs) constitute a concern to the environment when released into bodies of water because they are often only utilised once in wastewater treatment and are challenging to recover. The NPs can be incorporated in or supported by a polymeric matrix, like electro spun fibres, to reduce this risk [5]. Immobilising the NPs on these supports would enable the catalysts to be reused, so extending their useful lives.

2. Experimental

Nanocomposites have gained significant attention in various fields due to their unique properties and versatile applications. In this study, we focus on the preparation of nanocomposites using a polymer blend of polyvinyl-alcohol (PVA), polyethylene-glycol (PEG), polyvinylpyrrolidone (PVP), and titanium dioxide (TiO_2) nanoparticles. The optical properties of these nanocomposites are investigated, as they play a crucial role in potential applications such as optoelectronics and sensors [6].
The synthesis of titanium dioxide nanoparticles was carried out using the sol-gel method. In the first step, TiO_2 nanoparticles were prepared by a sol-gel process, where titanium precursor and stabilizing agents were mixed in a suitable solvent. The resulting solution was subjected to hydrolysis and condensation reactions, leading to the formation of TiO_2 nanoparticles [7]. Subsequently, the synthesized TiO_2 nanoparticles were calcined at two different temperatures, 400 °C and 700 °C, to optimize their crystalline structure and remove any residual organic species. Calcination is a crucial step that influences the morphology, size, and crystallinity of the nanoparticles, thereby affecting the overall properties of the nanocomposite. The prepared TiO_2 nanoparticles of concentration (1, 5, 10, 15, 20 and 25 wt%) (TiO_2) were then mixed with the polymer blend in specific weight ratios (PVA various wt%, PEG 10 wt% and PVP 5 wt%). The selection of PVA, PEG and PVP as the polymer components is based on their compatibility with the nanoparticles and their ability to form a stable composite system [8]. The weight ratios of the components were carefully chosen to ensure a homogeneous dispersion of the nanoparticles within the polymer matrix. The solvent casting method was employed to fabricate the nanocomposite [9]. The polymer blend and TiO_2 nanoparticle mixture were dissolved in a suitable solvent, followed by the casting of the solution onto a flat substrate. The solvent was evaporated under controlled conditions to obtain uniform nanocomposite with a desired thickness. The nanocomposite samples were subjected to optical characterization to investigate their optical properties. Optical characterization provides valuable insights into the interaction of light with the nanocomposite materials and allows for the analysis of their optical behavior.

3. UV-Vis spectroscopy studies

A UV-VIS spectrometer was employed to measure the optical parameters at room temperature in the wavelength range (200 - 1100) nm [10].

3.1 Optical properties

The ratio of the incident light intensity (I_0) to the intensity of the transmitted light (I_t) is known as the transmittance spectrum (T), and it is represented by the following equations [11]:

$$T = \frac{I_t}{I_0} = 10^{-A} \tag{1}$$

where: A is the absorbance, additionally, the thickness of the material, temperature, and filler method all affect transmittance [12]. Nevertheless, the inversion of the transmittance (T) is called absorbance (A), or the optical density, since the transmittance's negative logarithm is represented by the absorption, it can be written as follows:

$$A = \log T^{-1} \tag{2}$$

The type of material and the length of the incident radiation wave are two variables that have an impact on a material's absorption. Between 200 nm and 1100 nm, the absorbance was measured as a function of wavelength, in Figure 1 (a). It is noticed at $\lambda = 245$ nm less absorbance was 39.4% in concentration (without TiO_2) and higher absorbance was 98% in concentration 25 wt% TiO_2. And for the Figure 1 (b) it is noticed at $\lambda = 245$ nm less absorbance was 32.9% in concentration 1 wt% TiO_2 and higher absorbance was 86.3% in concentration 25 wt% TiO_2. Figure 1 demonstrates that the absorbance declines with increasing wavelength for all prepared samples. This can be explained physically by the inability of the incident photon to excite and move the electron from the valance band to the conduction band. Because the incident photon energy is lower than the nanocomposite's energy gap value, the absorbance is decreased by increasing the wavelength. Additionally, it is observed that absorbance decreases as the rate of filler increases, which supports the idea that the introduction of dopant material atoms into the prepared samples' crystalline structure caused the formation of local levels within the energy gap, which in turn caused the absorption of photons with low energies [13].
Photocatalysis is a chemical process in which a material (known as a photocatalyst) quickens a chemical reaction by absorbing and using light energy. Different photocatalytic materials can absorb light at various wavelengths or energies due to their diverse absorption spectra. While certain photocatalysts function best in the ultraviolet (UV) region, others can also be used in the visible or infrared spectrum [3].
At $\lambda = 350$ nm (ultraviolet) region of 20 wt% TiO_2 calcination 400 °C has the highest value of the photocatalytic in composite compared with other prepared sample, at $\lambda = 630$ nm (visible) region of 25 wt% TiO_2 calcination 400 °C has the highest value of the photocatalytic in composite compared with other prepared sample and at $\lambda = 1000$ nm (infrared spectrum) of 25 wt% TiO_2 calcination 400 °C has the highest value of the photocatalytic in composite compared with other prepared sample.
Figure 2 (a&b) depict the transmittance curve plotted as a function of wavelength for all prepared samples, and Eq. (1) was used to determine the transmittance values. From Figure 2 (a) we note that the transmittance decreases with increasing concentration of TiO_2, where the sample

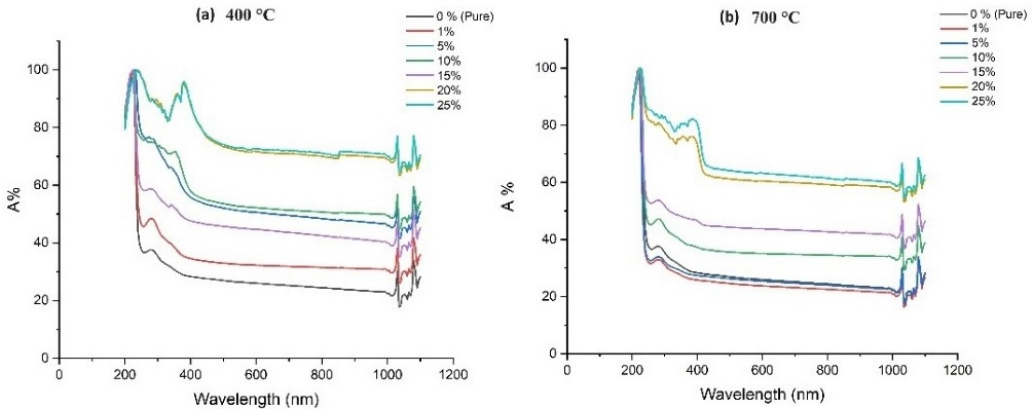

Figure 1. The absorbance spectra of prepared samples as a function of wavelength for calcination (a) 400 °C and (b) 700 °C.

of concentration (0 wt% TiO_2) yielded the maximum transmittance, at 400 °C calcination and less transmittance in concentration (25 wt% TiO_2) and from Figure 2 (b) we note that the sample with concentration (1 wt% TiO_2) had the maximum transmittance. At 700 °C calcination and less transmittance in concentration 25 wt% TiO_2, This is due to the filler's larger particle size compared to the matrix's smaller particle size, which increases absorption and decreases transmission and due to additives that reduce incident light at low wavelengths' ability to transmitting due to the layer form of covalent connections between polymer chains [14]. That shows the-fraction of light lost due to scattering. This outcome suggests that the TiO_2 packed atoms will modify the polymer's structure [15].

According to the energy conservation equation, we can determine the reflectance (R) based on the spectrums of transmittance (T) and absorbance (A) [16]:

$$R = 1 - (T + A) \tag{3}$$

Eq. (3) was used to calculate the reflectance from the absorbance and transmittance spectra using the energy conservation law. The reflectance of the prepared samples shown as a function of wavelength in Figure 3. In general, we found that as wavelength is increased, reflectance increases. The reflectance curves' apparent common behavior is to first show a reduction in reflectance value before rising with increasing wavelength. Between wavelengths (300 - 390 nm) and (400 - 1100 nm), there is a decrease, and then there is an increase. The amount of scattering in the UV-VIS reflectance spectrum is far less than the amount of absorption. The optical band gap, which corresponds to the rapid decrease in reflectance at a specific wavelength, indicates that the particles are almost consistently dispersed throughout the prepared specimen [17].

3.2 Optical constants

3.2.1 Absorption coefficient (α)

Materials' absorption coefficients are strongly correlated with both photon energy and band gap energy. It depends on the incident photon energy and the kind of electronic transitions that take place between the energy bands and can be defined as the attenuation in the flood of radiation energy or the intensity per unit of area in the direction of the wave in the medium [18]. The reason of the attenuation in incident photon energy is the absorption processes. where the following equation connects the absorbance with the absorption coefficient [19]:

$$\alpha = 2.303\left(\frac{A}{d}\right) \tag{4}$$

where d is the thickness, and α is the absorption coefficient. From Figure 4 (a) it is noticed at $\lambda = 245$ nm less value of

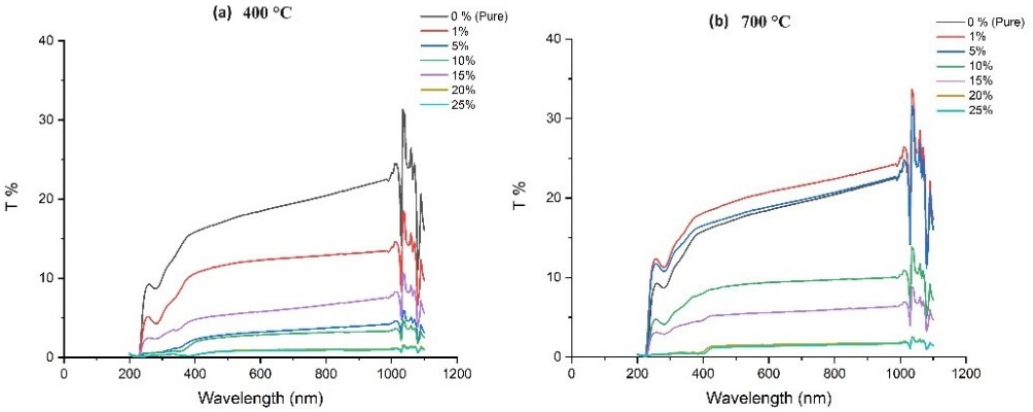

Figure 2. The transmittance spectra of prepared samples as a function of wavelength for calcination (a) 400 °C and (b) 700 °C.

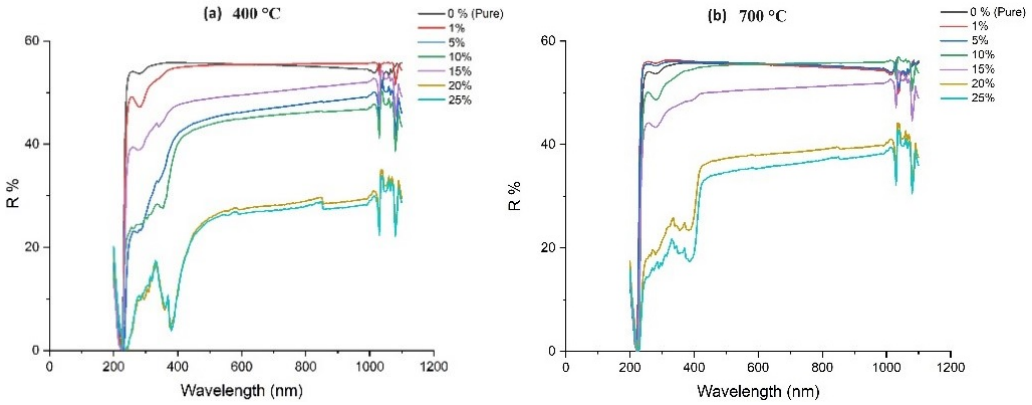

Figure 3. The Reflectance of prepared samples as a function of wavelength for calcination (a) 400 °C and (b) 700 °C.

absorption coefficient where it was 4.28 cm^{-1} (1 wt% TiO_2) and higher absorption coefficient was 16.17 cm^{-1} in concentration 25 wt% TiO_2. Extended states inside the energy gap and close to the conduction band could be the reason of this, which increase absorption of long-wavelength photons. High absorption means that there is a high chance that an electron will transition from the valence band to the conduction band when the incident photon energy is high.

In Figure 4 (b) shows the absorption coefficient α cm^{-1} as a function of wavelength for (Blend-TiO_2) nanocomposite. It is shows increase in the absorption coefficient with increasing concentration of TiO_2. It is noticed at $\lambda = 245$ nm Less value of absorption coefficient where it was 2.98 cm^{-1} (1 wt% TiO_2) and higher absorption coefficient was 13.72 cm^{-1}) in concentration 25% TiO_2. The absorption coefficient aids in determining the nature of electronic transitions. When the absorption coefficient is high ($\alpha > 10^4$ cm^{-1}) at high energies, we expect direct electronic transitions, and when the absorption-coefficient is low ($\alpha < 10^4$ cm^{-1}) at low energies, we expect indirect electronic transitions, which preserve the electron and photon's energy and momentum [20, 21]. The coefficient of absorption for the (Blend-TiO_2) nanocomposite is less than ($\alpha < 10^4$ cm^{-1}) that the electron transitions is indirect.

3.2.2 Extinction coefficient (K)

Extinction coefficient K is defined as the quantity of the energy absorbed in sample, or the extinction that happened in electromagnetic wave inside the material and by the following relation [22, 23]:

$$K = \frac{\alpha\lambda}{4\pi} \tag{5}$$

The extinction coefficient (K) was illustrated in Figure 5 (a) as a function of wavelength of the (Blend-TiO_2) nanocomposite at different concentration. The extinction coefficient has changed its behaviour, becoming more pronounced in the visible and near-infrared spectrums while becoming less pronounced at the low wavelength of the absorption edge. The extinction coefficient is associated with the absorption coefficient, and when the absorption coefficient increases, so the coefficient extinction increases with additive increased. Less value of the extinction coefficient (1 wt% TiO_2) at TiO_2 calcination 400 °C and higher the extinction coefficient was in concentration (25 wt% TiO_2) this was due to its lowest energy gap value.

In Figure 5 (b) shows the extinction coefficient (K) as a function of wavelength for (Blend-TiO_2) nanocomposite at different concentration. Also, it is shows increase in the extinction coefficient with increasing concentration of TiO_2 and from Figure 5 it show that the extinction coefficient in

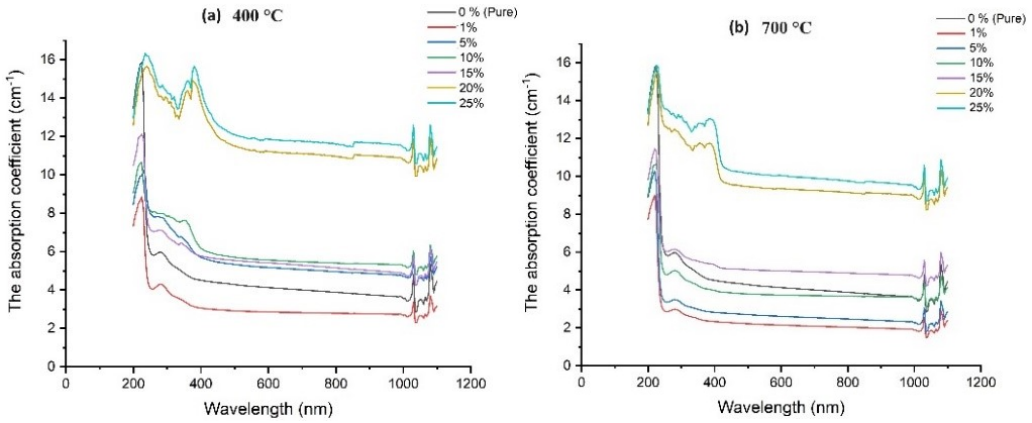

Figure 4. The Absorption coefficient (α) of prepared samples as a function of wavelength for calcination (a) 400 °C and (b) 700 °C.

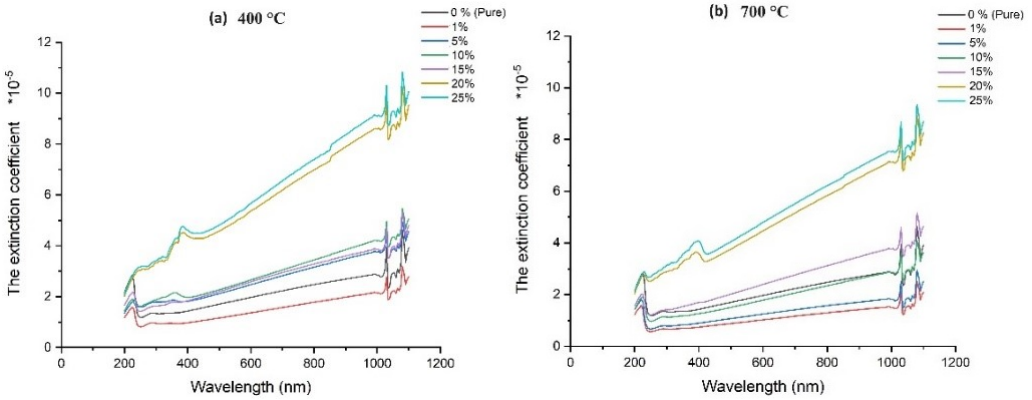

Figure 5. The extinction coefficient (K) of prepared samples as a function of wavelength for calcination (a) 400 °C and (b) 700 °C.

(Blend-TiO_2) nanocomposite for TiO_2 at calcination 400 °C higher than that of calcination 700 °C. Because of crystal structure for the TiO_2 phase anatase (400 °C calcination) and rutile (700 °C calcination) where the anatase phase has a tetragonal crystal structure. It is characterized by a distorted octahedral coordination of titanium atoms, resulting in a lower symmetry structure compared to rutile. While rutile phase has a more compact and dense tetragonal crystal structure. It consists of octahedrally coordinated titanium atoms in a more regular and symmetric lattice [24, 25].

3.2.3 Refractive index (n)

It can be characterized as the difference between the speed of light in a vacuum and the speed of a medium [26, 27]:

$$R = \frac{(n-1)^2 + K^2}{(n+1)^2 + K^2} \tag{6}$$

This equation allows us to determine the refractive index:

$$n = \sqrt{\left(\frac{1+R}{1-R}\right)^2 - (K^2+1)} + \frac{1+R}{1-R} \tag{7}$$

Figure 6 (a) shows refractive index for (Blend-TiO_2) nanocomposite as a function of wavelength at different concentration. The values of refractive index increased with the decrease of photon energy. This decrease indicates that the electromagnetic radiation passing through the material is slower in the low photon energy. A light beam becomes refractive when it passes through a dielectric substance. The physical explanation for this is because light moves at a different speed inside the dielectric. The refractive index is a parameter directly correlated to the density of material. A given material's less dense polymorphs will be more openly structured and hence lower than their denser equivalents. It is obvious from this Figure that the refractive index of the samples is influenced by increasing the filler percentage in TiO_2, that is related to increase the density of composite, this, in accordance with the Lorentz-Lorentz formula, is the outcome of an increase in the number of atomic refractions brought about by an increase in liner polarizability [28]. Refractive index values increased as photon energy decreased. This drop shows that electromagnetic radiation with low photon energy passes through the material more slowly [29].

However, at $\lambda = 1015$ nm the refractive-index of (Blend-TiO_2) nanocomposite for TiO_2 calcination 400 °C in (1 wt% TiO_2) concentration is (3.95) while the refractive index (n) for TiO_2 calcination 700 °C in (10 wt% TiO_2) concentration is (4). The refractive index of 10 wt% (TiO_2) calcination 700 °C, has the highest value in composite compared with other prepared sample that was explained by the fact that it reflected the greatest value.

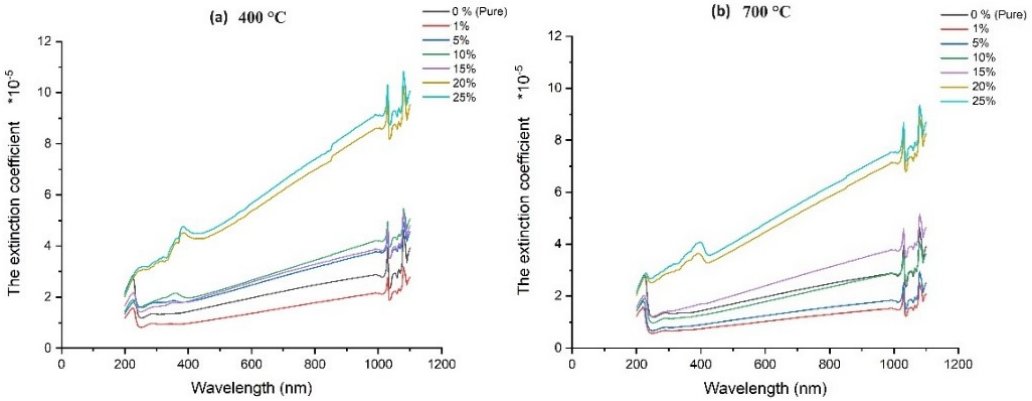

Figure 6. The refractive index (n) of prepared samples as a function of wavelength for calcination (a) 400 °C and (b) 700 °C.

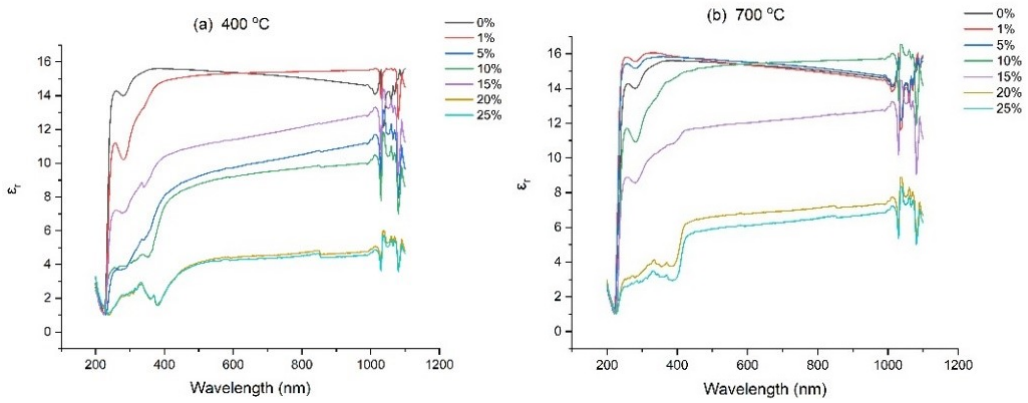

Figure 7. The dielectric constant real part (ε_r) of prepared samples as a function of wavelength for calcination (a) 400 °C and (b) 700 °C.

Calcination at 400 °C, TiO_2 undergoes a phase transition from the amorphous phase to the crystalline anatase phase. Calcination at 700 °C as the temperature increases, TiO_2 undergoes another phase transition, transforming from the anatase phase to the rutile phase. The refractive index of TiO_2 at 700 °C is higher than that of 400 °C due to the different crystalline structure of rutile. Depending on measurement conditions the index can vary slightly depending on factors such as impurities and particle size.

The-following equations describe (ε_r) and (ε_i) components of the dielectric constant:

$$\varepsilon_r = n^2 - K^2 \tag{8}$$

$$\varepsilon_i = 2nK \tag{9}$$

Eqs. (8) and (9) are used to determine the dielectric constant's (ε_r) and (ε_i) components.

Figure 7 shows dielectric constant real part (ε_r) for (Blend-TiO_2) nanocomposite as a function of wavelength at different concentration. At $\lambda = 1015$ nm the dielectric constant of real part (ε_r) of (Blend-TiO_2) nanocomposite for TiO_2 calcination 400 °C in (1 wt% TiO_2) concentration is (15.62) while the dielectric imaginary part (ε_i) for TiO_2 calcination 700 °C in (1 wt% TiO_2) concentration is (16.06). The dielectric constant of real part (ε_r) of 1% TiO_2 calcination 700 °C, has the highest value in composite compared with other prepared sample.

Figure 8 shows dielectric constant imaginary part (ε_i) for (Blend-TiO_2) nanocomposite as a function of wavelength at different concentration, at $\lambda = 1015$ nm the dielectric constant of imaginary part (ε_i) of (Blend-TiO_2) nanocomposite for TiO_2 calcination 400 °C in (25 wt% TiO_2) concentration is (4.36×10^{-4}) while the dielectric imaginary part (ε_i) for TiO_2 calcination 700 °C in (25 wt% TiO_2) concentration is (4.35×10^{-4}). The dielectric constant of imaginary part (ε_r) of 25 wt% TiO_2 calcination 400 °C, has the highest value in composite compared with other prepared sample.

At a higher calcination temperature of 700 °C, TiO_2 transitions from the anatase phase to the rutile phase. This change in crystal structure has a significant effect on the optical dielectric constant. The increase can be attributed to the alignment and rearrangement of atoms in the crystal lattice, leading to enhanced polarization and dielectric response.

3.2.4 Energy gap

The indirect energy gap of the prepared samples composite as a function of optical energy-gap $h\nu$. Optical band gap can be determined from absorption coefficient. We can determine the indirect optical energy gap by charting $(\alpha h\nu)^2$ against $h\nu$, the band-gap can be calculated by extrapolating the linear component of the curves to zero absorption value

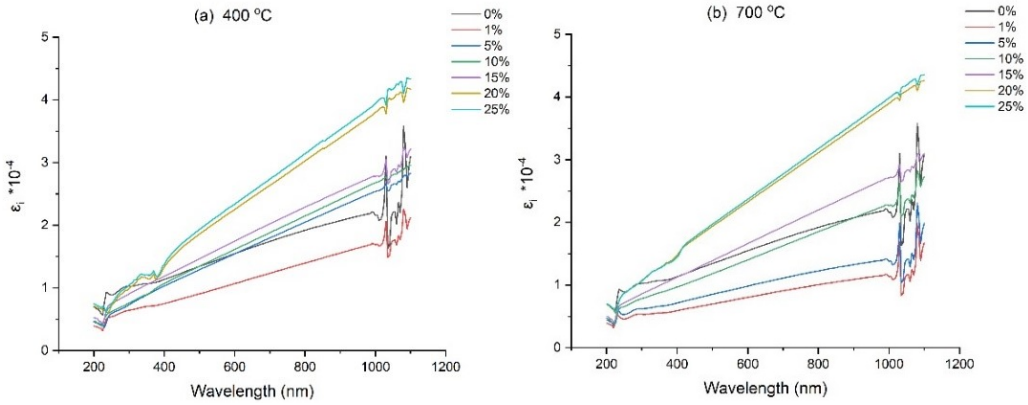

Figure 8. The dielectric imaginary part (ε_i) of prepared samples as a function of wavelength for calcination (a) 400 °C and (b) 700 °C.

and then finding the intercept on the energy axis. Table 1 presents the values of the indirect energy gap that were obtained [30].

Figure 9 shows that by rate of filler of PVA, PVP, and PEG components, the value of the permitted energy gap reduces. This indicates that the filler caused the absorption edge to shift towards the low energies, as seen in Figure 9. This drop can be explained by the filler generating levels in the energy gap and near the conduction band. Which led to the absorption of low energy photons. Table 1 contains the energy gap values for the permitted direct transition of prepared samples.

Table 1 indicates that an increase in filler concentration results in a decrease in the optical band gap. The crystal lattice's atom distribution and arrangement, as well as the composites' crystal structure, are the main determinants of the energy gap values, thus, the increase in disorder in the material is responsible for the decrease in the energy gap, On the other hand, defects of formation, such as voids, may arise during composite mixing and give birth to desired localized states in the material's band gap, furthermore, decrease in cluster size of the parent solution. Where the band

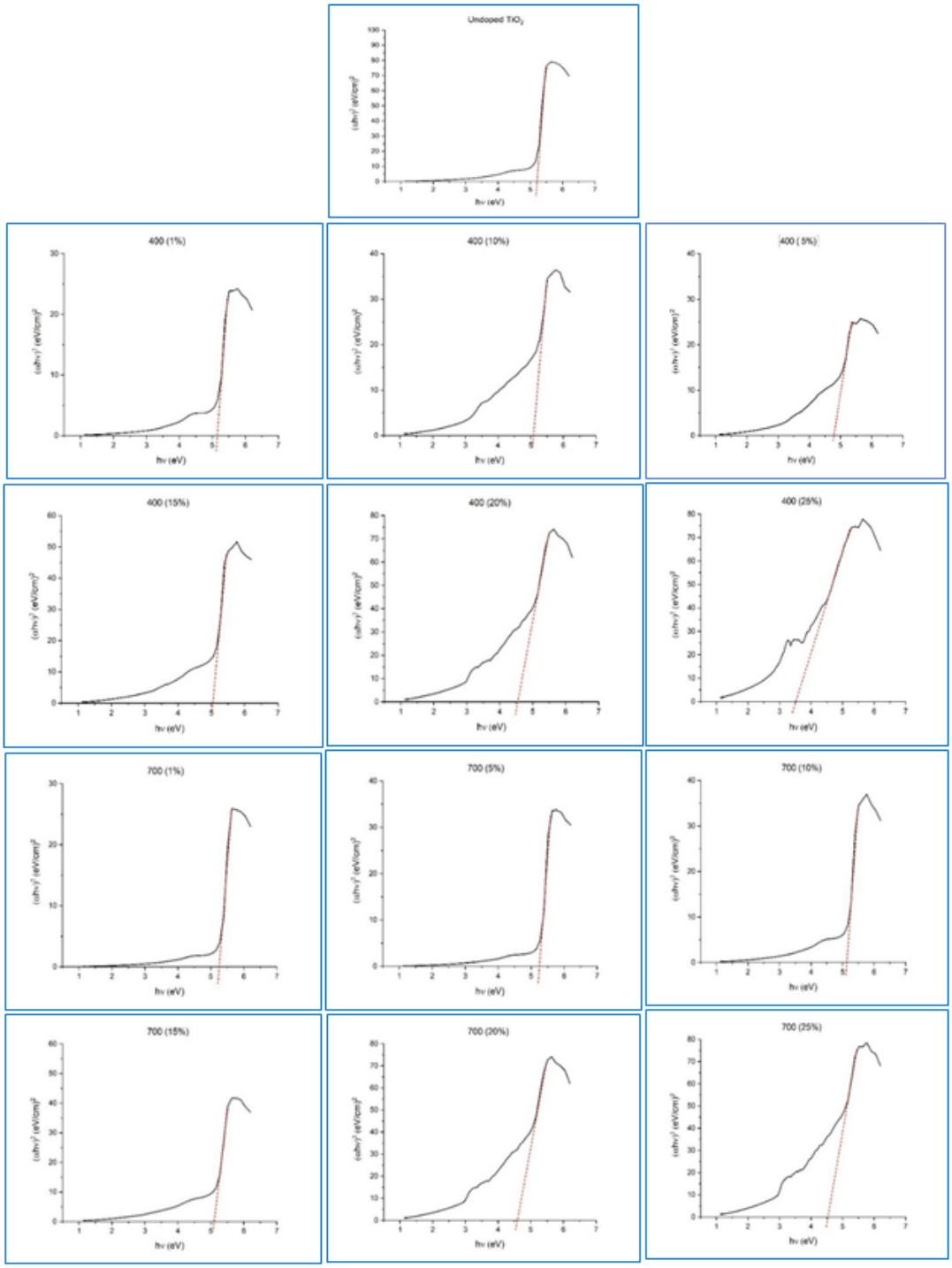

Figure 9. The prepared samples' optical band gaps as a function of wavelength.

Table 1. The calculated energy gap values of the samples that were prepared.

	Mixture Percentage (wt%)	Energy gap (eV)
Pure polymer	0	5.27
400	1	5.16
	5	4.81
	10	5.09
	15	5.03
	20	4.55
	25	3.51
700	1	5.25
	5	5.24
	10	5.14
	15	5.10
	20	4.59
	25	4.53

gap decreased from 5.27 eV to 3.51 eV. More imperfect sites were created on the TiO_2 surface as a result of the doped TiO_2 nanoparticles energy gap narrowing. These surface flaws have the qualified to absorb more visible light [30]. The increase in values of energy band gap at 10 and 15 wt% of TiO_2 may be due to porosity in nanocomposites can lead to more complex interactions with the photonic material. The presence of pores can create additional interfaces and surfaces within the material, which can scatter, absorb or reflect light differently compared to a solid nanocomposite. This can lead to modifications of the optical energy band gap.

4. Conclusion

The synthesis of nanocomposites (titanium dioxide nanoparticles) blended with (PVA various wt%, PEG 10 wt% and PVP 5 wt%) using the Sol-gel combustion process has been effectively shown. High absorption values of prepared samples.

Adding Nano titanium oxide (TiO_2) to polyvinyl alcohol (PVA) improves photocatalytic properties for water purification. TiO_2 in nano form has a larger surface area, enhancing its photocatalytic efficiency. When exposed to UV light, TiO_2 generates electron-hole pairs that react with water or contaminants, forming reactive oxygen species (ROS) that break down organic compounds. PVA supports TiO_2, prevents aggregation, and offers mechanical strength. The combination extends TiO_2 photocatalytic activity to visible light, using PVA to capture and transfer energy to TiO_2. This enhancement is valuable for various applications like water treatment and antibacterial surfaces.

The behavior of titanium dioxide nanoparticles and polymer dopant as substitutional impurity existing in the lattice position of TiO_2, certified the existence of unique phase of anatase TiO_2 nanoparticles. The represent a good optical property have led to reduce of band gap values for with the increase of filler percentage of TiO_2 nanoparticles from (20 to 25 wt%).

Ethical approval
This manuscript does not report on or involve the use of any animal or human data or tissue. So the ethical approval is not applicable.

Authors Contributions
All the authors have participated sufficiently in the intellectual content, conception and design of this work or the analysis and interpretation of the data (when applicable), as well as the writing of the manuscript.

Availability of data and materials
The datasets generated and analyzed during the current study are available from the corresponding author upon reasonable request.

Conflict of Interests
The author declare that they have no known competing financial interests or personal relationships that could have appeared to influence the work reported in this paper.

References

[1] G. Patel, M. B. Sureshkumar, and P. Patel. "Effect of TiO_2 on optical properties of PMMA: An optical characterization". *Adv. Mater. Res.*, **383**:3249–3256, 2012.

[2] C. B. Marien, C. Marchal, A. Koch, D. Robert, and

P. Drogui. "Sol-gel synthesis of TiO_2 nanoparticles: Effect of Pluronic P123 on particle's morphology and photocatalytic degradation of paraquat.". *Environ. Sci. Pollut. Res.*, **24**:12582–12588, 2017.

[3] X. Liu, Q. Chen, L. Lv, X. Feng, and X. Meng. "Preparation of transparent PVA/TiO_2 nanocomposite films with enhanced visible-light photocatalytic activity. ". *Catal. Commun.*, **58**:30–33, 2015.

[4] R. S. Al-Khafaji and F. Q. Mohammed. "Effect of catalysts on BN NanoParticles production.". *J. Mater. Res. Technol.*, **9**:868–874, 2020.

[5] I. R. Agool and A. Hashim. "Enhancement of structural and optical properties of (PVA-PVP-TiO_2) nanocomposites.". *Aust. J. Basic Appl. Sci.*, **8**, 2014.

[6] S. Mahshid, M. Askari, and M. S. Ghamsari. "Synthesis of TiO_2 nanoparticles by hydrolysis and peptization of titanium isopropoxide solution.". *J. Mater. Process. Technol.*, **189**:296–300, 2007.

[7] B. A. Jabbar, K. J. Tahir, B. M. Hussein, H. H. Obeed, N. J. Ridha, F. K. M. Alosfur, and R. A. Madlol. "Investigations on the nonlinear optical properties of Eu^{3+}: TiO_2 nanoparticles via Z-Scan technique.". *Mater. Sci. Forum*, **1039**:245–252, 2021.

[8] R. S. A. Al-Khafaji. "Synthesis and some features of three-phases polymer/metal/ceramic multilayers nanocomposite. ". *Ibn AL-Haitham J. Pure Appl. Sci.*, **33**:10–17, 2020.

[9] K. A. Jasim, M. A. Thejeel, and R. S. Al-Khafaji. "The effect of doping by Sr on the structural, mechanical and electrical characterization of $La_1Ba_{1-x}Sr_xCa_2Cu_4O_{8.5+\delta}$. ". *Ibn AL-Haitham J. Pure Appl. Sci.*, **27**:170–175, 2017.

[10] S. A. Fadaam, M. H. Mustafa, A. H. Abd AlRazaK, and A. A. Shihab. "Enhanced efficiency of CdTe photovoltaic by thermal evaporation vacuum.". *Energy Procedia.*, **157**:635–643, 2019.

[11] N. M. Al-Hada, A. M. Al-Ghaili, H. Kasim, M. A. Saleh, M. H. Flaifel, H. M. Kamari, H. Baqiah, J. Liu, and W. Jihua. "The effect of PVP concentration on particle size, morphological and optical properties of cassiterite nanoparticles. ". , *IEEE Access.*, **8**: 93444–93454, 2020.

[12] R. S. A. Al-Khafaji. "Synthesis of blend polymer (PVA/PANI)/Copper (1) oxide nanocomposite: thermal analysis and UV-Vis spectra specifications. ". *Iraqi J. Sci.*, :3888–3900, 2021.

[13] N. M. Ahmed, F. A. Sabah, H. I. Abdulgafour, A. Alsadig, A. Sulieman, and M. Alkhoaryef. "The effect of post annealing temperature on grain size of indium-tin-oxide for optical and electrical properties improvement. ". *Results Phys.*, **13**:102159, 2019.

[14] M. I. Rahmah, H. S. Majdi, W. K. Al-Azzawi, M. J. Rasn, H. H. Jasim, M. S. Jabir, R. A. S. A. Alkareem, and T. M. Rashid. "Synthesis of ZnO/Ag-doped C/N heterostructure for photocatalytic application.". *Int. J. Mod. Phys. B.*, :2350239, 2023.

[15] K. A. Jasim and R. S. Al-Khafaji. "The effect of oxygen flow on the transition temperature of $Hg_{0.75}Pb_{0.25}Sr_{2-y}Ba_yCa_2Cu_3O_{8+\delta}$ superconductors. ". *Phys. Conf. Ser.*, :012096, 2018.

[16] O. G. Abdullah and S. A. Hussen. "Variation of optical band gap width of PVA films doped with aluminum iodide.". *Adv. Mater. Res.*, **383**:3257–3263, 2012.

[17] S. M. Ali, A. A. Shehab, and S. A. Maki. "Study of the influence of annealing temperature on the structural and optical properties of ZnTe prepared by vacuum thermal evaporation technique.". *Ibn AL-Haitham J. Pure Appl. Sci.*, **31**:50–57, 2018.

[18] R. N. Abed, M. A. Sattar, S. S. Hameed, D. S. Ahmed, M. Al-Baidhani, M. Kadhom, A. H. Jawad, K. Zainulabdeen, M. H. Al-Mashhadani, and A. A. Rashad. "Optical and morphological properties of poly (vinyl chloride)-nano-chitosan composites doped with TiO_2 and Cr_2O_3 nanoparticles and their potential for solar energy applications. ". *Chem. Pap.*, **77**:757–769, 2023.

[19] S. M. Nejad, S. G. Samani, and E. Rahimi. "Characterization of responsivity and quantum efficiency of TiO_2—Based photodetectors doped with Ag nanoparticles. ". *2nd Int. Conf. Mech. Electron. Eng.*, **6**:382–394, 2010.

[20] Y. Xu, J.-H. Yang, S. Chen, and X.-G. Gong. "Defect-assisted nonradiative recombination in $Cu_2ZnSnSe_4$: A comparative study with Cu_2ZnSnS_4.". *Phys. Rev. Mater.*, **5**:025403, 2021.

[21] A. A. Mohaimeed and B. H. Rabee. "Influence of Berry dye on some properties of nanocomposite (PVA/TiO_2) films.". *Opt. Quantum Electron.*, **55**:254, 2023.

[22] V. A. Markel. "Extinction, scattering and absorption of electromagnetic waves in the coupled-dipole approximation. ". *J. Quant. Spectrosc. Radiat. Transf.*, **236**:106611, 2019.

[23] A. Z. Obaid, M. H. Mustafa, and H. K. Hassun. "Studying the effect of the annealing on Ag_2Se thin film.". *AIP Conf. Proc.*, , 2020.

[24] M. Curcio, A. De Bonis, S. Brutti, A. Santagata, and R. Teghil. "Pulsed laser deposition of thin films of TiO_2 for Li-ion batteries. ". *Appl. Surf. Sci. Adv.*, **4**: 100090, 2021.

[25] R. S. A. Al-Khafaji and K. A. Jasim. "Dependence the microstructure specifications of earth metal lanthanum La substituted $Bi_2Ba_2CaCu_{2-X}La_XO_{8+\delta}$ on cation vacancies.". *AIMS Mater. Sci.*, **8**:550–559, 2021.

[26] Y. Doubi, B. Hartiti, M. Siadat, Y. Arba, M. Stitou, H. Labrim, H. J. T. Nkuissi, S. Fadili, M. Tahri, and P. Thevenin. "Impact of indium ions on some properties of TiO2 thin films for sensor applications.". *Mater. Today Proc.*, **66**:385–389, 2022.

[27] A. Seetharaman, D. Sivasubramanian, V. Gandhiraj, and V. R. Soma. "Tunable nanosecond and femtosecond nonlinear optical properties of C–N–S-doped TiO_2 nanoparticles.". *J. Phys. Chem. C.*, **121**: 24192–24205, 2017.

[28] A. H. Ahmad and A. M. Awatif. "Dopping effect on optical constants of polymethylmethacrylate (PMMA). ". *Eng. Technol. J.*, **25**, 2007.

[29] R. Tintu, K. Saurav, K. Sulakshna, V. P. N. Nampoori, P. Radhakrishnan, and S. Thomas. "$Ge_{28}Se_{60}Sb_{12}$/PVA composite films for photonic applications. ". *J. Non-Oxide Glas.*, **2**:167–174, 2010.

[30] R. John and R. Rajakumari. "Synthesis and characterization of rare earth ion doped nano ZnO. ". *Nano-Micro Lett.*, **4**:65–72, 2012.